

03.5

Excitation of a capillary wave as a mechanism for the formation of pores in the process of deep penetration by laser radiation

© R.D. Seidgazov, F.Kh. Mirzade

Institute on Laser and Information Technologies Branch of the Federal Scientific Research Center „Crystallography and Photonics“, Russian Academy of Sciences, Shatura, Moscow region, Russia
E-mail: seidgazov@mail.ru, fmirzade@rambler.ru

Received March 14, 2023

Revised April 27, 2023

Accepted April 27, 2023

The mechanism of pore formation due to the capture of gas bubbles in the process of excitation of low-frequency capillary waves and alternating collapses in the cavity under laser action is studied experimentally. It is shown that bubble capture is provided by the main vibrational mode, the wavelength of which is related to the cavity depth as $\lambda = 4L/3$.

Keywords: laser radiation, deep penetration, capillary waves, keyhole pore formation.

DOI: 10.61011/TPL.2023.06.56384.19553

The deep penetration regime is characterized by the emergence of a hollow cavity within which laser radiation propagates deeper, shaping an elongated and narrow melting zone. The features of this regime are being studied extensively for application in additive assembly of parts from metallic powders by selective laser melting. Porosity induced by surface waves of liquid metal in a cavity makes it impossible to realize fully the advantages of deep penetration. Recoil pressure due to evaporation of a fraction of the liquid phase volume [1,2] or thermocapillary flows in the melt [3,4] are the causes of melt deformation. Technological quality standards impose restrictions on the evaporation intensity, thus establishing the dominance of the thermocapillary mechanism [5–8] and making it necessary to study the generation of pores by capillary waves. The diversity of concepts regarding excited surface vibrational modes renders it difficult to gain a clear insight into the dynamics of pore generation and necessitates experimental determination of the main mode. The aim of the present study is to examine the mechanism of pore formation in a cavity under stationary continuous laser action. The excitation of capillary waves at the cavity walls in a model experiment on penetration of paraffin by laser radiation with a power of 30 W (performed in accordance with the procedure outlined in [5]) was observed for this purpose. The optical transparency of molten paraffin facilitates visual observation of the melting boundary and hydrodynamic processes in the cavity at the second stage of its evolution, which starts after its rapid growth at the first stage and ends prior to inflow and vanishing of the cavity under continuing irradiation (the third stage). The diagram of the experiment is presented in Fig. 1, *a*. Figure 1, *b* shows waves (with a frequency of 16 Hz) in a thin molten layer on the walls of a 5-mm-deep cavity. Owing to a „scissor effect“ the axial amplitude at the bottom of the cavity reaches 40% of its

depth. Short-term cavity collapses with bubble capture were observed.

The images in Fig. 1, *b* are indicative of excitation of a capillary wave with wavelength λ being proportional to cavity depth L and comparable to it ($\lambda \approx L$). This is in line with the assumptions made in [5]. The main mode in relation $L = (2n + 1)\lambda/4$ ($n = 0, 1, 2, 3, \dots$) corresponds to $\lambda = 4L/3$ at $n = 1$. Cavity collapses with bubble capture occur when the peaks of waves from opposite cavity walls come into contact (see the schematic diagram for a cylindrical cavity in Fig. 2). The following four qualitatively different phases may be identified in vibration cycles of the free surface of melt.

Phase 1. Waves develop after the ejection of melt from the inlet of a cavity, which has reached its ultimate depth L , ceases. Thermocapillary forces, which are directed radially from the most heated region on the laser beam axis, displace the liquid layer from the cavity bottom, shifting it upward along the walls. As it rises up, the flow velocity decreases with diminishing surface temperature gradient and increasing cross-section of the liquid layer (in accordance with the mass conservation condition). At a certain height H_1 , the flow velocity drops to zero and liquid mass accumulates in the form of a wave peak.

Phase 2. The growth of a wave peak at height H_1 induces local detachment of the viscous sublayer from the melting boundary, and a return near-wall flow forms. In a deep cavity with a shape coefficient in excess of $L/D \approx 3$ (ratio of the depth of a cavity to its width), peaks of waves block laser radiation, thus reducing the temperature at the cavity bottom and weakening the surface temperature gradient and the thermocapillary force (i.e., blocking of radiation facilitates cavity collapse).

Phase 3. Wave peaks may come into contact (i.e., cavity collapse with bubble capture may occur) if the wave reaches a sufficient amplitude in a deep cavity with

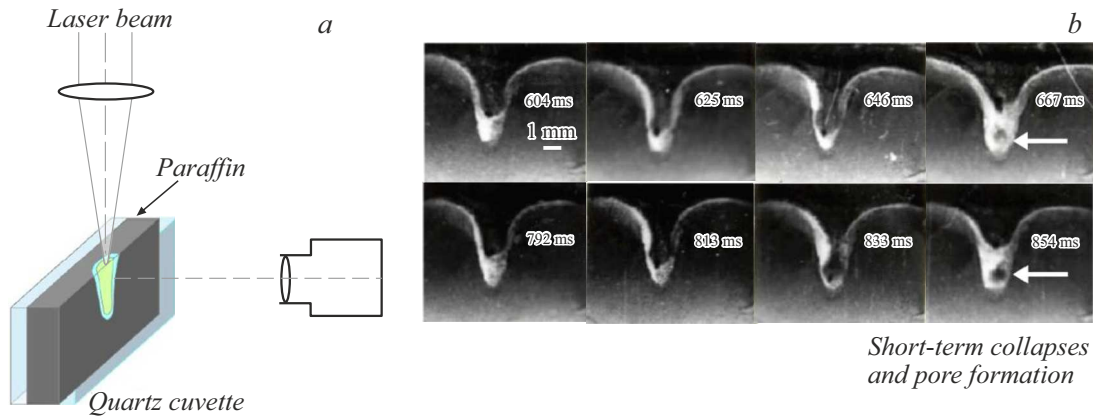


Figure 1. *a* — Diagram of the experiment. *b* — Capillary waves in a penetration cavity in paraffin. Short-term collapses with gas bubble capture are indicated with arrows.

$L/D \approx 3$ or more. According to the diagram, the distance between the cavity bottom and the point of contact of wave peaks is approximately equal to one half of the wavelength: $H_1 = \lambda/2 = 2L/3$.

Phase 4. In the conditions of single-spot long-term laser action, a gas bubble manages to leave the melt before the onset of the next cycle of surface vibrations.

The linear theory of excitation of capillary waves in deep metal caverns due to the development of thermocapillary instability and the prerequisites for their emergence have been examined quantitatively in [4]. Presenting the liquid metal on the cavity walls in the form of a cylinder with inner and outer radii a and b (Fig. 2) and assuming that the frequencies of axial and azimuthal capillary waves excited at the inner cavity surface are close to the frequency of ordinary capillary waves in a uniformly heated liquid layer [9], one may write the following expression:

$$\Omega_m^2 = \frac{\sigma k}{\rho a^2} (k^2 a^2 + m^2) E_m, \quad (1)$$

where Ω_m is the frequency of mode m of capillary waves; σ and ρ are the surface tension and the density of molten metal, respectively; k is the wave number; m is the azimuthal number; $k = 2\pi/\lambda = (2n + 1)\pi/2L$; and $E_m = E_m(k, a, b)$ is a coefficient that depends on wave number k and cavity parameters a and b :

$$E_m(k, a, b) = \frac{|I'_m(kb)K'_m(ka) - I'_m(ka)K'_m(kb)|}{I'_m(kb)K_m(ka) - I_m(ka)K'_m(kb)},$$

where $I_m(ka)$ and $K_m(ka)$ are modified Bessel functions of the first and second kind and order m (prime mark denotes the derivative of a function with respect to argument). Cyclic frequency $\omega = 2\pi f$ (f is the frequency in Hz). In the case of long capillary waves with the distance of emergence of perturbations being much greater than the thickness of melt on the cavity walls and comparable to cavity depth L (at $kh \ll 1$, $h = b - a$), relation (1) for the frequency of an axially symmetric mode ($m = 0$)

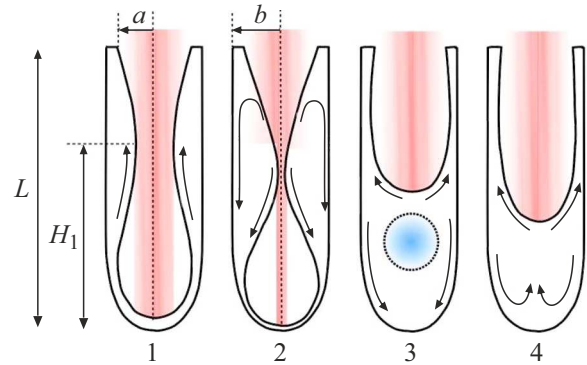


Figure 2. Diagram of phases 1–4 of surface vibrations and gas bubble capture in a penetration cavity.

of melt vibrations $\Omega_0 = \omega(k)$ takes the following form: $\omega^2 = (\sigma/\rho)k^4 h$. Setting $\lambda = 4L/3$, we find the dependence of the vibration frequency (in Hz) on depth L and thickness h of the molten layer:

$$f = \frac{1.125\pi}{L^2} \sqrt{\frac{\sigma h}{\rho}}. \quad (2)$$

Inserting the parameters of paraffin ($\rho = 8 \cdot 10^2 \text{ kg/m}^3$, $\sigma = 0.025 \text{ N/m}$) and a vibration frequency of 16 Hz into (2), we find $h = 0.4 \text{ mm}$, which corresponds to the images in Fig. 1, *b*.

The needed data for a metal target are provided by supplement Movie S1 from [10], which details the process of penetration of titanium alloy Ti–6Al–4V by laser radiation with a power of 156 W focused to a spot $140 \mu\text{m}$ in size. The excitation of vibrations with a frequency on the order of 40 kHz, which are accompanied by bubble capture, was detected when the cavity depth reached $75 \mu\text{m}$. Using these data and setting $\rho = 4 \cdot 10^3 \text{ kg/m}^3$ and $\sigma = 1.4 \text{ N/m}$ for titanium at high temperatures, we obtain $h = 11.5 \mu\text{m}$ from (2). This estimate is verified by simplified expression $h \approx \chi/V$ (χ is the temperature

conductivity and V is the cavity growth rate) [2]. Quantity V is estimated based on the data from [10] for the first period of vibrations: $V = Af$, where A is the depth change (axial amplitude) within period $1/f$. Thickness h for temperature conductivity $\chi \approx 9 \cdot 10^{-6} \text{ m}^2/\text{s}$ of titanium, axial amplitude $A \approx 2.5 \cdot 10^{-5} \text{ m}$ of the first period of vibrations, and a frequency of 40 kHz is $9 \mu\text{m}$. The obtained value is close to the earlier estimate of $11.5 \mu\text{m}$.

In actual technological processes, the time scale of solidification of metals is short relative to the time of bubble removal (under the influence of thermocapillary effect forces or buoyancy forces); therefore, a pore may form when the laser action ceases. Note that laser beam scanning may disrupt the axial symmetry of a cavity and intensify the influence of other vibrational modes. This needs to be examined in further studies.

Conflict of interest

The authors declare that they have no conflict of interest.

References

- [1] J.G. Andrews, D.R. Atthey, *J. Phys. D: Appl. Phys.*, **9** (15), 2181 (1976). DOI: 10.1088/0022-3727/9/15/009
- [2] V. Semak, A. Matsunawa, *J. Phys. D: Appl. Phys.*, **30** (18), 2541 (1997). DOI: 10.1088/0022-3727/30/18/008
- [3] N. Postacioglu, Ph. Kapadia, J. Dowden, *J. Phys. D: Appl. Phys.*, **22** (8), 1050 (1989). DOI: 10.1088/0022-3727/22/8/007
- [4] V.I. Ledenev, F.Kh. Mirzade, *Quantum Electron.*, **23** (12), 1030 (1993). DOI: 10.1070/QE1993v023n12ABEH003278.
- [5] R.D. Seidgazov, Yu.M. Senatorov, *Sov. J. Quantum Electron.*, **18** (3), 396 (1988). DOI: 10.1070/QE1988v018n03ABEH011530.
- [6] R.D. Seidgazov, in *2019 IEEE 8th Int. Conf. on advanced optoelectronics and lasers (CAOL)* (Sozopol, Bulgaria, 2019), p. 216. DOI: 10.1109/CAOL46282.2019.9019431
- [7] R.D. Seydgazov, F.Kh. Mirzade, *Welding Int.*, **35** (7-9), 359 (2021). DOI: 10.1080/09507116.2021.1979829.
- [8] S. Ly, G. Guss, A.M. Rubenchik, W.J. Keller, N. Shen, R.A. Negres, J. Bude, *Sci. Rep.*, **9**, 8152 (2019). DOI: 10.1038/s41598-019-44577-6
- [9] F.Kh. Mirzade, A.M. Zabelin, *Izv. Ross. Akad. Nauk. Ser. Fiz.*, **63** (10), 2025 (1999) (in Russian).
- [10] R. Cunningham, C. Zhao, N. Parab, Ch. Kantzos, J. Pauza, K. Fezzaa, T. Sun, A.D. Rollett, *Science*, **363** (6429), 849 (2019). DOI: 10.1126/science.aav4687

Translated by D.Safin